Attorney Docket No. 8793-52026 **PATENT**

IN THE UNITED STATES PATENT AND TRADEMARK OFFICE

In Re Application Of: Bellaiche, L., et al.

Appl. No.: 10/632,740 Group Art Unit: 1755

Filed: 08/01/2003 Examiner: Koslow, C.

For: Enhanced Electromechanical Properties in Atomically-Ordered Ferroelectric Alloys

Commissioner for Patents
P.O. Box 1450
Alexandria, VA 22313-1450

DECLARATION UNDER 37 CFR 1.132

Laurent Bellaiche declares as follows:

1. I am one of the joint inventors of the invention described and claimed in the referenced patent application.

2. Tabata, H. et al., Formation of artificial $BaTiO_3/SrTiO_3$ superlattices using pulsed laser deposition and their dielectric properties, Appl. Phys Lett 65 (15), 1970-72, 10 October 1994 (attached hereto as Exhibit A) discloses the preparation of barium titanate/strontium titanate superlattices by pulsed laser deposition.

3. Zhao, T. et al., Enhancement of second-harmonic generation in $BaTiO_3/SrTiO_3$ superlattices, Phys. Rev. B, 60 (3), 1697-1800, 15 July 1999 (attached hereto as Exhibit B) discloses the preparation of barium titanate/strontium titanate superlattices by molecular beam epitaxy.

4. Exhibits A and B show that it was known to those skilled in the art at the time the present application was filed that it is possible to grow superlattices using these techniques without forming the disordered alloy.

5. The alloys described in Exhibits A and B and the alloy of the present invention differ in that in the former case the individual layers would not be ionically charged while the individual layers are ionically charged in the modulated alloy of the present invention. Christen, H.-M. et al., The growth and properties of epitaxial $KNbO_3$ thin films and $KNbO_3/KTaO_3$ superlattices, Appl. Phys. Lett. 68 (11), 1488-90, 11 March 1996 (attached hereto as Exhibit C) discloses the growth of potassium niobate/tantalate superlattices by PLD. In potassium niobate/tantalate superlattices, the layers are alternately charged –1 and +1. Therefore, superlattices may be grown even when the layers are ionically charged.

6. I further declare that all statements made herein of my own knowledge are true and that all statements made on information and belief are believed to be true; and further that these statements were made with the knowledge that willful false statements and the like so made are punishable by fine or imprisonment, or both, under Section 1001 of Title 18 of the United States Code, and that such willful false statements may jeopardize the validity of the above-referenced application or any patent issuing thereon.

Date: 04/25/06

Laurent Bellaiche

Formation of artificial $BaTiO_3/SrTiO_3$ superlattices using pulsed laser deposition and their dielectric properties

Hitoshi Tabata, Hidekazu Tanaka, and Tomoji Kawai
The Institute of Scientific and Industrial Research, Osaka University, 8-1 Mihogaoka, Ibaraki, Osaka 567 Japan

(Received 18 February 1994; accepted for publication 1 August 1994)

We have formed strained dielectric superlattices of $BaTiO_3$ (BTO) and $SrTiO_3$ (STO) by a pulsed laser deposition technique. A large strain of 400–500 MPa is introduced at the interface between the BTO and STO layers. A large dielectric constant of 900 was observed with a stacking periodicity of 2 unit cells/2 unit cells. The superlattices show drastically different electrical behavior from that of the solid solution $(Sr,Ba)TiO_3$ films. Broad maxima of the dielectric constants occur around 40–50 °C and the values remain large even for a temperature above 200 °C. © *1994 American Institute of Physics.*

Barium titanate ($BaTiO_3$) is one of the most important ferroelectric perovskites. Therefore, a large number of studies have been performed to elucidate the mechanism giving rise to the ferroelectricity of this material and to improve the properties.[1] To enhance the ferroelectric behavior of $BaTiO_3$, for example, various kinds of cations have been substituted for Ba and Ti. In particular, when Ba is replaced by Sr as a solid solution, the dielectric constant increase dramatically.[2] Isostatic pressure is also effective to enhance the dielectric constant.[3,4] In the case of films, the formation of superlattices, approach to artificially control the ferroelectric properties. With this approach, atoms such as Ba and Ti in $BaTiO_3$ can be replaced site selectively and strain can be introduced by a combination of different layers. Here, we report for the first time the observation of novel super-dielectric properties in strained superlattices of $BaTiO_3$ and $SrTiO_3$.

The tetragonal form of $BaTiO_3$ exhibits ferroelectric distortions involving displacements of the cations (Ti^{4+}, Ba^{2+}) relative to the anions (O^{2-}), leading to a net dipole moment per unit volume. These soft-mode distortions correspond to a 1% *c* axis/*a* axis lattice strain in tetragonal $BaTiO_3$ [Fig. 1(a)]. When $BaTiO_3$ layers (called BTO hereafter) are combined with $SrTiO_3$ layers (called STO hereafter) as BTO/STO superlattices, there is a relatively large mismatch of 3.0% between the in-plane lattice parameters (BTO; 3.990 Å, STO; 3.905 Å). Thus strain is induced by changing the periodicity of the strained superlattices [Fig. 1(b)]. In order to study the importance of the soft-mode coupling with the lattice strain, ferroelectric strained superlattice is also effective, because even in cases with small strain in BTO, the strain energy strongly affects the phase transition as was indicated in the bulk sample.[5]

In this study, the BTO and STO layers were stacked alternately by a multitarget pulsed laser deposition technique. This technique offers advantages for film growth, including epitactic growth at low substrate temperatures; congruent deposition of materials with complex stoichiometries and facile deposition of materials with high melting points.[6,7] An ArF excimer laser beam was focused onto the target of BTO and STO alternately with an energy density of 500 mJ/cm^2, and the BTO and STO layers were deposited layer-by-layer on conductive Nb doped single-crystal $SrTiO_3(100)$ substrates. The thickness of each layer was varied in the range from 4 Å (1 unit cell) to 1000 Å (250 unit cell) and the total thickness of the superlattices was fixed at 2000 Å. The films were formed at 650 °C in an oxygen/ozone (8%) ambient at a pressure of 3 mTorr. The deposition rate was 10–15 Å/min.

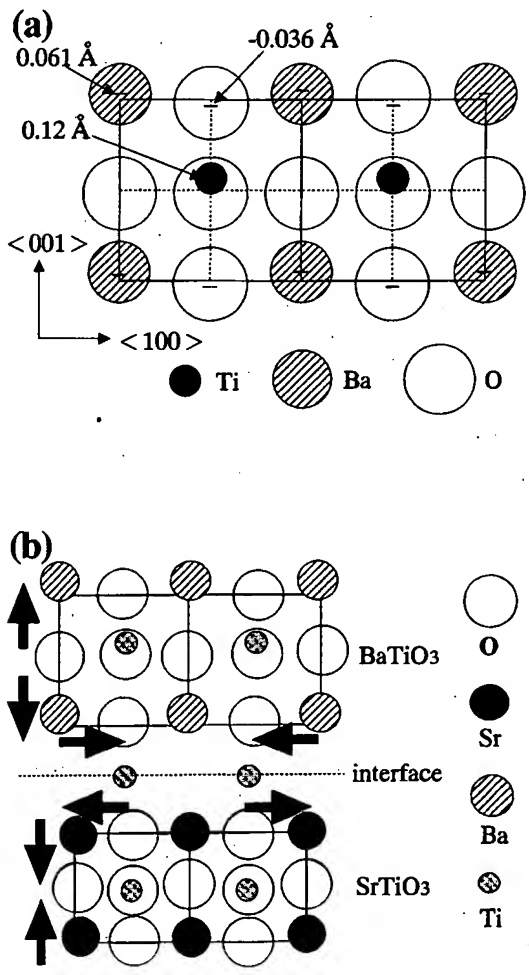

FIG. 1. (a) A schematic model of ferroelectric distortion in $BaTiO_3$ crystal. (b) Stress occurs at the interface between BTO and STO layers due to the large lattice mismatch.

 0003-6951/94/65(15)/1970/3/$6.00

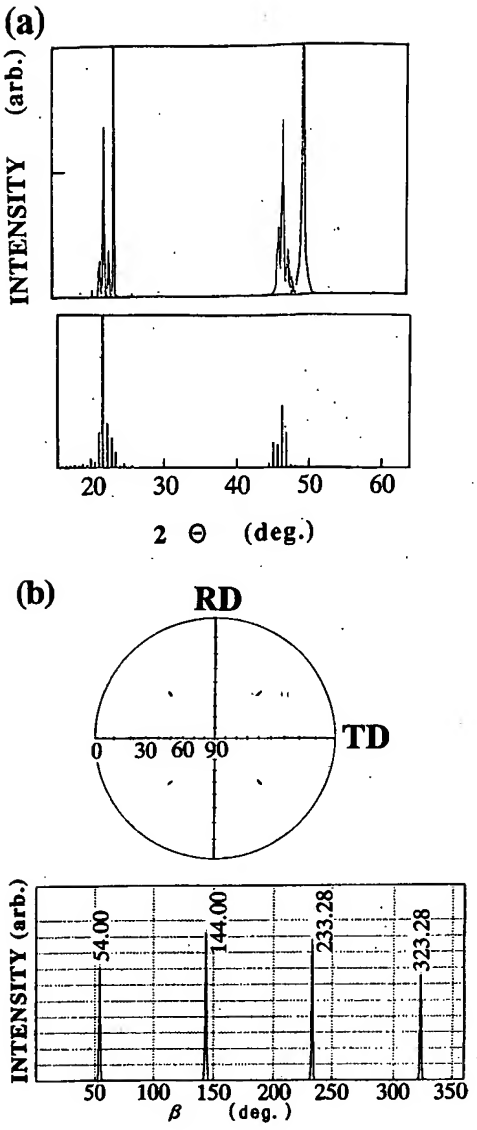

FIG. 2. (a) The x-ray diffraction pattern of BTO (20 Å)/STO (20 Å) superlattice and calculated one with the stacking periodicity of 5 unit cells (20 Å). (b) The pole figure and x-ray diffraction scans of BTO layer in the BTO/STO superlattice with the stacking periodicity of 20 unit cells (500 Å).

The lattice parameters of the films were measured by 2θ-θ x-ray diffraction and four circle x-ray diffraction methods. The dielectric constants (ϵ_r) of the films were measured with *LCR* meters at temperatures betwen 20 to 200 °C.

Figures 2(a) and 2(b) show the θ-2θ x-ray diffraction pattern and the pole figure with scan pattern of BTO (20 Å)/STO (20 Å) superlattice, respectively. The diffraction pattern indicates that the BTO/STO superlattice was formed as designed, and the pole figure and β scan patterns indicate that the STO and BTO films are in complete epitaxy with the substrate.

Figure 3(a) shows the variation of the ratio of lattice constant c and a of the STO and BTO layers as a function of the periodicity of each layer. The lattice parameter c of the BTO layers increases with decreasing stacking periodicity below 250 (1000 Å)/250 (1000 Å) unit cells. On the other hand, the lattice constant a decreases with decreasing periodicity, just opposite of lattice constant c [Fig. 3(b)]. Thus the expansion of c axis in the BTO layers is attributed to an in-plane pressure effect due to the large lattice mismatch between the BTO and STO layers. The pressure induced by the STO layers is estimated to be about 400–500 MPa from elastic calculations. The changes of the lattice parameters a and c saturate at a stacking periodicity of approximately 40 Å (10 unit cells). In this range, the superstructures can also be observed in the x-ray diffraction patterns; that is, the combination of main peaks with satellite peaks [Fig. 2(a)]. Therefore, crystallographically, these superlattices should be classified as new materials having a longer c-axis length.

The changes in the dielectric constant (ε_r) of the BTO/STO superlattices as a function of the stacking periodicity are shown in Fig. 4(a). ε_r does not change much for periodicities between 100 and 1000 Å (25–250 unit cells cycle). In the range between 100 Å (25 unit cells) and 8 Å (2 unit cells) stacking, however, ε_r increases with decreasing stacking periodicity. It is well known that the dielectric constants of the BTO , and BSTO decrease with decreasing the film thickness.[8–13] It should be noted that the ε_r of $(Sr_{0.5},Ba_{0.5})TiO_3$ solid solution thin films decreases monotonously below a film thickness of 2000 Å and becomes almost zero at a thickness of 250 Å [Fig. 4(a)]. In the case of the

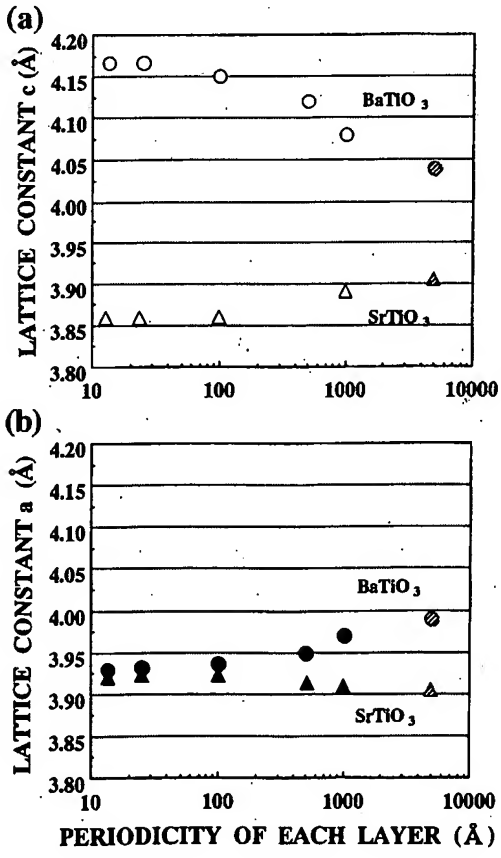

FIG. 3. Variation of the ratio of the lattice constant a and c of BTO (○,●) and STO (△,▲) layers in the STO/BTO superlattices against the layer thickness of each stacking periodicity. The total thickness of these superlattices is 2000 Å. Shaded circles and triangles show the lattice constant a and c of single phase films with thickness of 5000 Å.

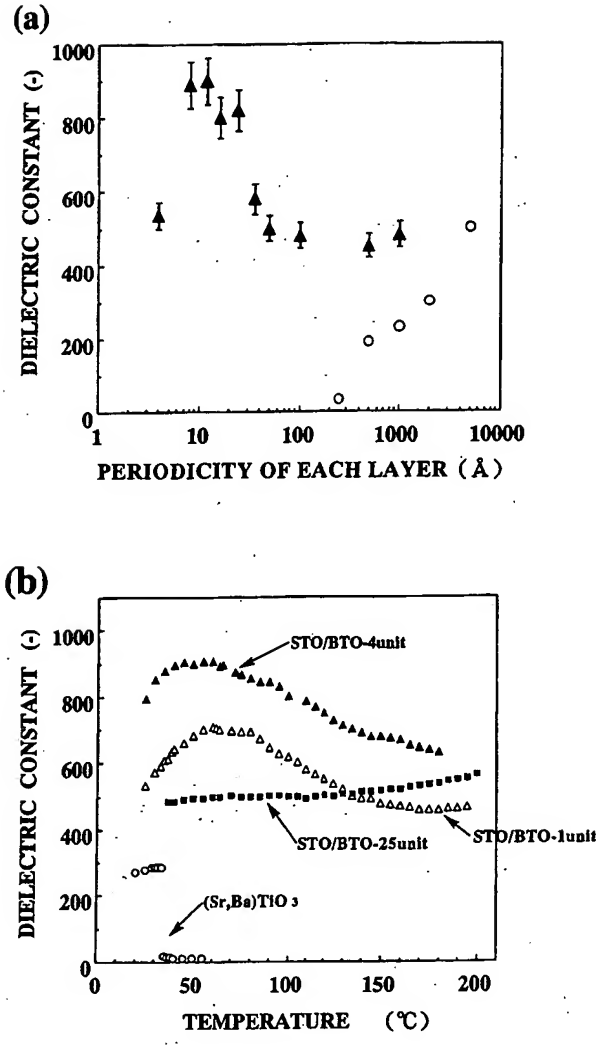

FIG. 4. (a) Dielectric constants of BTO/STO superlattice (▲) and $(Sr_{0.5},Ba_{0.5})TiO_3$ (○) vs stacking periodicity. (b) Temperature dependence of dielectric constant (ε_r) of various BTO/STO superlattices (total thickness is 2000 Å). (1) △: STO/BTO—1 unit cell stacking; (2) ▲: STO/BTO—4 unit cell stacking; (3) ■: STO/BTO—25 unit cell stacking; and (4) ○: $(Sr,Ba)TiO_3$ solid solution film (10 kHz, at 25 °C).

changing the total thickness of superlattices (from 2000 to 500 Å), the ε_r are maintained high value in the stacking periodicity of 4/4 unit cells. The results will be reported in details in the future. Considering these tendencies, the superlattice structure and the stress caused at the interface between the STO and BTO layers, apparently, play an important role in the enhancement of the dielectric constant. At the one unit cell periodicity, ε_r decreases 500. Presumably this because is caused by the fact that, in this 1/1 structure, the TiO_2 layer is sandwiched between a BaO and SrO layer. This type of crystal structure is quite similar to that of $(Sr_{0.5},Ba_{0.5})TiO_3$ solid solutions in the sense that both Sr and Ba are included in the basic perovskite cell. In the case of superlattices with larger than 2/2 stacking periodicity, an original crystal structure of BTO is maintained for each unit cell; that is, TiO_2 is sandwiched between two BaO layers. Therefore, the crystal structures of the 1/1 and 2/2 superlattices are essentially different. The temperature dependence of ε_r at 10 kHz shows particularly interesting behavior as indicated in Fig. 3. The ε_r of $(Sr_{0.5}Ba_{0.5})TiO_3$ solid solution thin films becomes zero at 35 °C because of the phase transition from the tetragonal to the cubic structure. For the BTO/STO superlattices, on the other hand, a broad peak of ε_r, which is a typical feature of ferroelectric films, is observed around 50–60 °C and high ε_r values are kept even at temperatures higher than 200 °C in the 1/1 and 4/4 superlattices. This indicates that the ferroelectric phase transition occurs at high temperature for the superlattice. Furthermore, for the BTO/STO (25–100 units) superlattices, the ε_r value increases with temperature up to 200 °C. [The Curie temperature of simple BTO is known as around 130 °C (Refs. 14–16).] The tetragonal phase of BTO may become stable due to the compressive in-plane stress induced by the STO layers. We believe that these phenomena observed in these particular superlattices should be called "super-dielectric properties" which are artificially induced by a chosen layering sequence.

In the "soft-mode" model, the atoms primarily occupy the ideal cubic sites at high temperatures. As the temperature is lowered, one of the transverse optical (TO) modes softens and becomes unstable, and the crystal transforms in the tetragonal phase with atomic displacements along the [001] direction.[17] In the case of these strained superlattices, the soft mode may be frozen in by the compressive stress in the BTO layers.

In conclusion, we have formed dielectric superlattices of STO/BTO using a pulsed laser deposition technique. The dielectric properties of the superlattices show considerably different behaviors from those of $SrTiO_3$, $BaTiO_3$, and $(Sr_{0.5},Ba_{0.5})TiO_3$ single phase films. The formation of dielectric and ferroelectric superlattices forms a promising approach for creating new super-ferroelectric materials and for study of the mechanism giving rise to ferroelectricity.

[1] R. E. Cohen, Nature **358**, 136 (1992).
[2] E. N. Bunting, G. R. Shelton, and A. S. Creamer, J. Am. Ceram. Soc. **30**, 114 (1947).
[3] R. Amirez, M. F. Lapena, and J. A. Gonzalo, Phys. Rev. B **42**, 2604 (1990).
[4] D. L. Decker and Y. X. Zhao, Phys. Rev. B **39**, 2432 (1989).
[5] S. Marais, V. Heine, C. Nex, and E. Salje, Phys. Rev. Lett. **66**, 2480 (1991).
[6] A. Wailenhorst, C. Doughty, X. X. Xi, S. N. Mao, Q. Li, T. Venkatesan, and R. Ramesh, Appl. Phys. Lett. **60**, 1744 (1992).
[7] H. Tabata, T. Kawai, and S. Kawai, Phys. Rev. Lett. **70**, 2633 (1993).
[8] K. Torii, T. Kaga, K. Kushida, H. Takeuchi, and E. Takeda, Jpn. J. Appl. Phys. **30**, 3562 (1991).
[9] Y. Hamada, Oyobutsuri **49**, 783 (1980).
[10] J. K. Panitz, J. Vac. Sci. Technol. **16**, 315 (1979).
[11] K. Srenivas, A. Mansingh, and M. Sayer, J. Appl. Phys. **62**, 4475 (1987).
[12] D. Roy and S. B. Krupanidi, Appl. Phys. Lett. **62**, 1056 (1993).
[13] M. N. Kamalasanan, N. P. Kumar, and S. Chandra, J. Appl. Phys. 5679 (1993).
[14] K. R. Carroll, J. M. Pond, D. B. Chrisey, J. S. Horwitz, R. E. Lenchtner, and K. S. Grabowski, Appl. Phys. Lett. **62**, 1845 (1993).
[15] M. G. Norton, P. B. Cracknell, and C. B. Carter, J. Am. Ceram. Soc. **75**, 1999 (1992).
[16] B. S. Kwak, Z. Zhang, E. P. Boyd, A. Erbil, and B. J. Wilkans, J. Appl. Phys. **69**, 767 (1991).
[17] J. Harada, J. D. Axe, and G. Shirane, Phys. Rev. B **4**, 155 (1971).

Enhancement of second-harmonic generation in $BaTiO_3/SrTiO_3$ superlattices

Tong Zhao, Zheng-Hao Chen,* Fan Chen, Wen-Sheng Shi, Hui-Bin Lu, and Guo-Zhen Yang
Laboratory of Optical Physics, Institute of Physics, Center for Condensed Matter Physics, Chinese Academy of Sciences, P.O. Box 603, Beijing 100080, People's Republic of China
(Received 16 February 1999)

Second-harmonic generation (SHG) of a 1.064-μm incident beam was investigated on $BaTiO_3/SrTiO_3$ superlattices prepared by laser molecular-beam epitaxy. The incidence angle and the polarization angle dependence of the SHG coefficients were measured. The SHG coefficients were greatly enhanced by the superlattice structure with the maximum value of $d_{33}=156.5$ pm/V being more than one order of magnitude larger than that of bulk $BaTiO_3$ crystal. The mechanism of SHG enhancement was discussed. [S0163-1829(99)02527-8]

To meet the need of the advanced electronic devices, many efforts have been made to enhance the dielectric and ferroelectric properties of ferroelectric materials with small dimensions. Being one of the most important ferroelectric perovskites, barium titanate ($BaTiO_3$) has attracted much attention. Recently, it has been found that the formation of the artificial superlattice of $BaTiO_3/SrTiO_3$ provided a powerful method for creating a new high-dielectric-constant material.[1,2] By stacking ferroelectric $BaTiO_3$ (BTO) and paraelectric $SrTiO_3$ (STO) alternately, the dielectric constant ε_r were greatly enhanced and the high ε_r values were kept around a broad range of both total thickness and temperature because of the in-plane stress resulting from the lattice mismatch between BTO and STO. Besides its large ferroelectric and dielectric response, BTO is also a good optical nonlinear material. According to optical nonlinear principles, high refractive, i.e., high dielectric materials should have large nonlinear susceptibilities. Therefore, one can predict that the BTO/STO superlattice should exhibit large optical nonlinearity, which has the promise for applications in optical switches, filters, waveguides, and electro-optic devices. To our knowledge, however, little work has been done on nonlinear optical properties of the BTO/STO superlattice.

In the present work, we investigated the characteristics of the second-harmonic generation (SHG), the fundamental phenomenon in nonlinear optical effect, of a series of BTO/STO superlattices with various stacking periodicities n/m, where n and m are the numbers of BTO and STO unit-cell layer in one BTO(n)/STO(m) period, respectively, and found that the periodical structure enhances SHG greatly.

In this study, the BTO and STO layers were stacked alternately by a multitarget laser molecular-beam epitaxy (LMBE) technique. An XeCl excimer laser beam (308 nm, 20 ns, 2 Hz) was focused on the sintered BTO, or single crystal STO targets alternately with the pulsed energy intensity of about 1 J/cm^2. Monitored by the reflection high-energy electron diffraction (RHEED), the BTO or STO layers were deposited layer by layer on single-crystal $SrTiO_3$ (100) substrates. The deposition rate was about 0.01 nm/pulse. The thickness of each BTO or STO layer was varied in the range from 0.8 nm (2 unit cells) to 20 nm (50 unit cells) and the total thickness of the superlattices were fixed at 80 nm (200 unit cells). The films were grown at 630 °C at an oxygen pressure of 1×10^{-4} Pa.

Crystallographic orientation and crystallinity of the deposited thin films were analyzed by either *in situ* RHEED patterns and the oscillations of their intensities or *ex situ* x-ray diffraction (XRD) patterns, atomic force microscopic (AFM), and high-resolution transmission electron microscopic (HRTEM) images. These results indicated that highly c-axis oriented BTO/STO superlattices were formed as designed with the root-mean-square roughness of 0.1 nm in surfaces and interfaces and in complete epitaxy with the substrates. Figure 1 shows the cross-sectional HRTEM micrograph of two periods of a BTO(20 unit cells)/STO(10 unit cells) superlattice, where there are 20 BTO unit cells and 10 STO unit cells in one period.

SHG data were collected using a typical setup with a signal and a reference channel.[3] The TEM_{00} output of a Q-switched Nd:YAG (yttrium aluminum garnet) laser with a wavelength of 1.064 μm was used as the fundamental beam. The laser pulse was incident on the superlattice mounted on a rotation stage, with a repetition rate of 5 Hz, a pulse duration of 20 ns, and a maximum energy of 50 mJ. The fundamental beam was split to pass through the signal and reference channels simultaneously. A piece of Z-cut quartz crystal (reference) was used in the reference channel for normalization against possible laser fluctuations. Another piece of

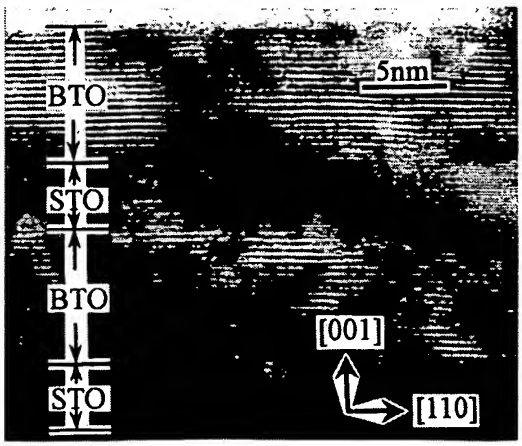

FIG. 1. Cross-sectional HRTEM micrograph of two periods of a BTO(20 unit cells)/STO(10 unit cells) superlattice.

Z-cut quartz crystal (calibration) was substituted for the superlattice specimen in the signal channel to allow the second-harmonic (SH) intensity from the superlattice to be scaled to the SHG coefficient $d_{11}=0.34$ pm/V of quartz. Selected by an analyzer placed before the photodetector, the p-polarized transmitted SH beam at 532 nm was measured as functions of both the incidence angle and the polarized angle of the fundamental beam. Each measured datum was obtained by a photomultiplier tube and by averaging the results of 100 laser shots using an instantaneous computer recording system. The thickness of the superlattice films (80 nm) was more than one order of magnitude less than the coherence length (3 μm) of bulk BTO;[4] hence the coherent factor in determining SHG coefficients can be ignored. Then the effective SHG coefficients for the superlattices can be approximately given by[4]

$$d_{\text{eff}} \approx \frac{l_q}{l_s}\left[\frac{n(2\omega)n^2(\omega)I_sT_q}{n_q(2\omega)n_q^2(\omega)I_qT_s}\right]^{1/2} d_{11}^q, \tag{1}$$

where $l_q=20\ \mu$m is the coherence length of quartz,[3] l_s is the superlattice thickness, $n(2\omega)$ and $n(\omega)$ are the refractive indices of the superlattice at SH and fundamental frequencies, respectively, $n_q(2\omega)$ and $n_q(\omega)$ are the refractive indices of the quartz at each of the frequencies, I_s and I_q are the normalized SH intensities, T_s and T_q are the transmission factors for the superlattices and the calibration quartz, respectively, and $d_{11}^q=0.34$ pm/V is the optical nonlinear coefficient of quartz.[3] According to our measurements, $T_s/T_q=0.8$. The refractive indices of BTO are similar to those of STO. So, we choose the refractive indices of BTO thin films as those of the BTO/STO superlattices, $n(2\omega)=2.2$, $n(\omega)=2.1$,[5] $n_q(2\omega)n_q^2(\omega)=3.7$.[6]

By assuming the BTO/STO superlattices have approximately the same structure symmetry ($4mm$) of the bulk BTO crystal, the second-order nonlinear polarization can be expressed as

$$P^{\text{NL}}=\begin{pmatrix} 0 & 0 & 0 & 0 & d_{15} & 0 \\ 0 & 0 & 0 & d_{15} & 0 & 0 \\ d_{31} & d_{31} & d_{33} & 0 & 0 & 0 \end{pmatrix}\begin{pmatrix} E_x^2 \\ E_y^2 \\ E_z^2 \\ 2E_yE_z \\ 2E_zE_x \\ 2E_xE_y \end{pmatrix}. \tag{2}$$

Figures 2(a)–2(f) show the fundamental polarization dependence of effective SHG coefficients for a series of BTO/STO superlattices with stacking periodicity $n/m=2/2$, 4/4, 10/10, 20/20, 30/30, and 50/50 unit cells, respectively. The incidence angle of the fundamental beam was chosen as 45° and the SH beam was p-polarized. The circle symbols represent experimental data. The solid lines are the best fits to the following function:

$$d_{\text{eff}}=|P^{\text{NL}}|/E^2=d_1\sin^2\theta+d_2\cos^2\theta, \tag{3}$$

which can be derived from Eq. (2), where θ denotes the angle between the fundamental polarization and the incidence plane, d_1 and d_2 are linear functions of d_{15}, d_{31}, and d_{33}. The nearly perfect fits indicate that the assumption of the BTO/STO superlattice with the same structure symmetry ($4mm$) of the bulk BTO is reasonable and these superlattices are isotropic in the plane of films. It should be noted that the maximum $|d_{\text{eff}}|$ values are much higher than the typical ones obtained from BTO films [2.13 pm/V (Ref. 4) and 0.8 pm/V (Ref. 5)].

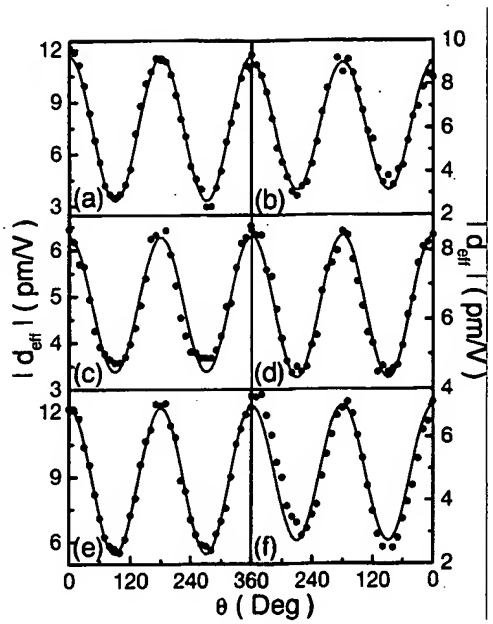

FIG. 2. Fundamental polarization dependence of the effective SHG coefficients of BTO/STO superlattices, with (a)–(f) being responsible for the stacking periodicity $n/m=2/2$, 4/4, 10/10, 20/20, 30/30, and 50/50 unit cells, respectively. The incidence angle of the fundamental beam was chosen as 45°. The SH beam was p polarized. The circle symbols represent experimental data. The solid lines are the best fits to Eq. (3).

To obtain the experimental values of d_{15}, d_{31}, and d_{33} for BTO/STO superlattices, the effective SHG coefficients as functions of the incidence angle α of the fundamental beam were measured. The fundamental and SH beams were selected as p-polarized. The results of $|d_{\text{eff}}|$ versus α are shown in Figs. 3(a)–3(f), which are responsible for the stacking periodicity $n/m=2/2$, 4/4, 10/10, 20/20, 30/30, and 50/50 unit cells, respectively. The circle symbols represent experimental data. The zero values of $|d_{\text{eff}}|$ at the zero incidence angles are the characteristics of the c-axis oriented BTO films. The solid lines are the best fits to the following function:

$$d_{\text{eff}}=d_{15}\sin 2\alpha_\omega\cos\alpha_{2\omega} + (d_{31}\cos^2\alpha_\omega+d_{33}\sin^2\alpha_\omega)\sin\alpha_{2\omega}, \tag{4}$$

which can be derived from Eq. (2). Here α_ω and $\alpha_{2\omega}$ are the internal angles of fundamental and SH beams, respectively, which are given by $n(\omega)\sin\alpha_\omega=\sin\alpha=n(2\omega)\sin\alpha_{2\omega}$ with $n(\omega)$ and $n(2\omega)$ being the refractive indices at the fundamental and SH frequencies, respectively. The fitting results of d_{15}, d_{31}, and d_{33} for a series of BTO/STO superlattices with various stacking periodicities are listed in Table I, where those values of the bulk BTO crystal and the BTO thin film obtained by other authors[6] are included for comparison.

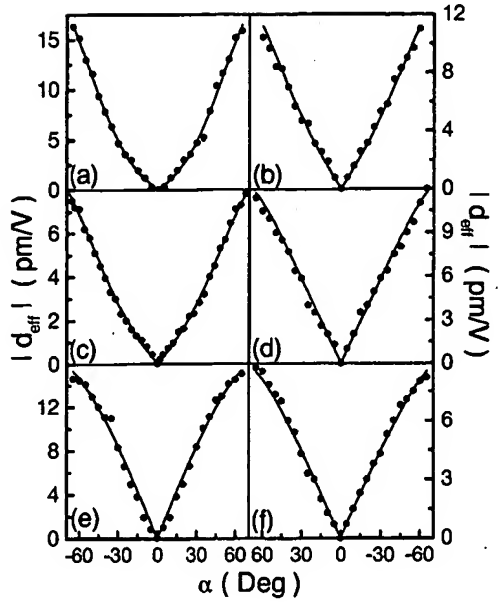

FIG. 3. Fundamental incidence angle dependence of the effective SHG coefficients of BTO/STO superlattices, with (a)–(f) being responsible for the stacking periodicity $n/m=2/2$, 4/4, 10/10, 20/20, 30/30, and 50/50 unit cells, respectively. The fundamental and SH beam were p polarized. The circle symbols represent experimental data. The solid lines are the best fits to Eq. (4).

From the fitting results, we can see that, for BTO/STO superlattices with various stacking periodicities, d_{15} is lower than that of the bulk BTO crystal, d_{31} is almost the same as, and d_{33} is much larger than those of the bulk BTO crystal, while they are all much larger than the typical BTO thin-film values reported by other authors. It should be noted that d_{33} has been dramatically enhanced with the maximum value being more than one order of magnitude larger than that of the bulk BTO crystal and it increases with decreasing the stacking periodicity.

The results above clearly show that the formation of the BTO/STO superlattice greatly enhances SHG from BTO. The enhancement can be attributed to several factors.

Bulk BTO has a perovskite-type tetragonal structure with point-group symmetry $4mm$, which is responsible for its ferroelectric and second-order optical nonlinear properties. Bulk STO has a cubic structure with point-group symmetry $m3m$, which is responsible for its paraelectric and non-second-order optical nonlinear properties. The lattice constants of bulk BTO and STO are $a=b=0.3990$ nm, $c=0.4036$ nm, and $a=b=c=0.3905$ nm, respectively.[1] Therefore, inside the BTO/STO superlattice, compression (expansion) and expansion (compression) stress are expected to be introduced along the interface and perpendicular to the interface in BTO (STO) layers resulting from the lattice mismatch between BTO and STO. So, in the c-axis oriented superlattices, the c axis was enlarged while the a axis was shortened for BTO layers. The lattice constant c of the BTO layers increases, while the lattice constant a decreases with decreasing stacking periodicity and reach their extremum values at the stacking periodicity $n/m=2/2$ unit cells. That is, a large stress ($\sim 10^9$ Pa)[1] was introduced into the BTO layers. Resulting from this stress, the tetragonal phase of BTO was stabilized, the spontaneous polarization $\mathbf{P}_s$ was increased, and the dielectric constant ε_r of BTO was enhanced with the same tendency as that of the lattice constant c and having the maximum value of 900 at the 2 unit cell/2 unit cell structure. The coefficient of SHG, d_{ijk}, can be expressed as $d_{ijk} \propto \chi_{ii}^{2\omega}\chi_{jj}^{\omega}\chi_{kk}^{\omega}$, where χ^{ω} and $\chi^{2\omega}$ are the linear optical susceptibilities at frequencies of ω and 2ω, respectively,[7] and $\chi=(\varepsilon_r-1)/4\pi$. So one can deduce that d_{ijk} was enhanced with the same tendency as that of ε_r.

In addition to the spontaneous polarization $\mathbf{P}_s$, the large stress in the BTO/STO superlattice can also produce an additional polarization $\mathbf{P}$ through the piezoelectric effect, which would produce SHG in the same way as does the spontaneous polarization $\mathbf{P}_s$.[5] $\mathbf{P}$ normal to the film surface would produce c-axis-oriented-like SHG. Using the stress given above and piezoelectric coefficients from Ref. 8, the value of $\mathbf{P}$ normal to the film surface produced by the stress in BTO layers through piezoelectric effect can be estimated to about 0.2 C/m^2, which is comparable with that of $\mathbf{P}_s$ in bulk BTO crystal,[9] 0.25 C/m^2. Hence, SHG may be enhanced by the stress in BTO layers through the piezoelectric effect.

Considering the enhancement of spontaneous and stress-induced polarizations and the enlargement of lattice constant of BTO layers being in the direction of c axis, the anisotropic enhancement of d_{15}, d_{31}, and d_{33} can be understood. The SHG coefficient d_{ijk} is proportional to the ensemble average of $r_i r_j r_k$, with r_i being the dipole moment operator in the i direction. Therefore, one should expect for the largest enhancement in $d_{33}(d_{ccc})$, and the small ones in $d_{15}(d_{aca})$ and $d_{31}(d_{caa})$.

Besides the contribution of polarization, the enhancement of SHG can also be attributed to the interfaces in BTO/STO superlattices. It has been found that the interfaces can produce SHG even in centrosymmetry semiconductor superlattices.[10] One can expect that the interfaces in BTO/STO superlattices may be responsible for a part of SHG.

Besides the explanation mentioned above, there may be two other reasons responsible for the enhancement of SHG. The first is the contribution of STO layers in BTO/STO superlattices. The bulk STO crystal is cubic, which cannot generate SH. In the BTO/STO superlattice, however, STO layers also strained due to the lattice mismatch. Without centrosymmetry, the strained STO layers may also generate SH. The second is the good crystallinity of the samples. As confirmed by XRD, AFM, and HRTEM, the BTO/STO superlattices

TABLE I. SHG coefficients of various BTO/STO superlattices with various stacking periodicities.

Stacking periodicity n/m (unit cells)	d_{15} (pm/V)	d_{31} (pm/V)	d_{33} (pm/V)
2/2	2.3	8.5	156.5
4/4	3.1	12.0	76.8
10/10	1.1	7.3	55.6
20/20	4.5	14.9	46.6
30/30	9.3	17.3	38.6
50/50	4.2	10.8	27.0
BTO bulk crystal	17.0	15.7	6.8
BTO thin film	2.2	2.1	0.90

used in this study were in complete epitaxy with the substrates with the root-mean-square roughness of only 0.1 nm in surfaces and interfaces, which may allow the superlattice thin films perform as single crystal.

From the discussion above, one can see that there are two conflicting factors affecting SHG in BTO/STO superlattices. The smaller the stacking periodicity was, the larger the stress and the polarization were introduced into the BTO layers, and the more the interfaces were involved, which can enhance SHG. On the other hand, the smaller the stacking periodicity was, the more the deviation of the BTO layers were from the bulk structure, which can reduce SHG. The resultant SHG is the balance of these two factors, which is responsible for the varying tendency in d_{33} and the aniostropic enhancement among d_{15}, d_{31}, and d_{33}.

In conclusion, BTO/STO superlattices with various stacking periodicities were grown by LMBE. The fundamental polarization dependence and the incidence angle dependence of SHG from these superlattices have been measured systematically. The data of experiments and theoretical fitting show that the SHG coefficients, especially d_{33}, were greatly enhanced by the formation of the BTO/STO superlattice with the maximum value being more than one order of magnitude larger than that of the bulk BTO crystal. The enhancement of SHG has been attributed to the enhancement of polarization, the introduced interfaces, the contribution of strained STO layers, and the good crystallinity. From the results above, it indicates that the BTO/STO superlattice may be very promising for nonlinear optical applications.

This work was supported by the Ministry for Science and Technology of China.

*Electronic address: zhchen@aphy.iphy.ac.cn

[1] Hitoshi Tabata and Tomoji Kawai, Appl. Phys. Lett. **70**, 321 (1997).

[2] Hitoshi Tabata, Hidekazu Tanaka, and Tomoji Kawai, Appl. Phys. Lett. **65**, 1970 (1994).

[3] H. A. Lu, L. A. Wills, B. W. Wessels, W. P. Lin, T. G. Zhang, G. K. Wong, D. A. Neumayer, and T. T. Marks, Appl. Phys. Lett. **62**, 1314 (1993).

[4] Bipin Bihari, Jayant Kumar, Gregory T. Stauf, Peter C. Van Buskirk, and Cheol Seong Hwang, J. Appl. Phys. **76**, 1169 (1994).

[5] L. D. Rotter, D. L. Kaiser, and M. D. Vaudin, Appl. Phys. Lett. **68**, 310 (1996).

[6] Tatsuo Okada, Yoshiki Nakata, Hiroshi Kaibara, and Mitsuo Maeda, Jpn. J. Appl. Phys., Part 2 **34**, L1536 (1995).

[7] Y. R. Shen, *The Principles of Nonlinear Optics* (Wiley, New York, 1984), p. 37.

[8] T. Ikeda, E. Nakamura, S. Nomura, E. Sawaguchi, Y. Shiozaki, and K. Toyoda, in *Numerical Data and Functional Relationships in Science and Technology*, edited by K.-H. Hellwege and A. M. Hellwege, Landolt-Börnstein, New Series, Group III, Vol. 3 (Springer-Verlag, Berlin, 1981), p. 55.

[9] M. DiDomenico, Jr. and S. H. Wemple, J. Appl. Phys. **40**, 720 (1969).

[10] Xudong Xiao, Chun Zhang, A. B. Fedotov, Zhenghao Chen, and M. M. T. Loy, J. Vac. Sci. Technol. B **15**, 1112 (1997).

The growth and properties of epitaxial $KNbO_3$ thin films and $KNbO_3/KTaO_3$ superlattices

H.-M. Christen,[a] L. A. Boatner, J. D. Budai, M. F. Chisholm,
L. A. Géa, P. J. Marrero,[b] and D. P. Norton
Solid State Division, Oak Ridge National Laboratory, Oak Ridge, Tennessee 37831

(Received 20 November 1995; accepted for publication 11 January 1996)

Potassium niobate ($KNbO_3$) thin films and potassium niobate/tantalate ($KNbO_3/KTaO_3$) superlattices have been grown on $KTaO_3$ (001) substrates by pulsed laser deposition. The thin-film structures were analyzed by Rutherford backscattering/ion-channeling techniques, x-ray θ–2θ and Φ scans, and both conventional and Z-contrast scanning transmission electron microscopy. Excellent film flatness and crystallinity are evidenced by these techniques. At room temperature, the $KNbO_3$ films are characterized by an orthorhombic structure which differs from that of bulk $KNbO_3$. The interfaces between the layers in the $KNbO_3/KTaO_3$ superlattice structures were found to be compositionally sharp on an atomic scale. © *1996 American Institute of Physics.*
[S0003-6951(96)03811-5]

Para- or ferroelectric properties in insulating perovskites can be drastically altered by small structural changes introduced either through defect-induced distortions or by external mechanical stresses. In the first case, a spatially random substitution of one ion for another of a slightly different ionic radius may result in ferroelectric[1] or "glassy" polar states.[2] In the case of an externally applied stress, the possibilities for inducing changes in a bulk sample are somewhat limited,[3] but surface tension can lead to a loss of ferroelectricity in fine-grained ceramics.[4] Similar behavior was observed in free-standing thin films,[5] but it was difficult to distinguish between the effects of mechanical constraints and depolarization fields due to surface-charge effects.

Heterostructures of alternating para- and ferroelectric thin films offer an interesting alternative. A superlattice in which one of the two materials changes its structure due to the "clamping" effect of the neighboring films may exhibit novel properties. Additionally, if a given ferroelectric structure exists over a range of film thicknesses, then size effects in ferroelectrics can be studied without being masked by the previously noted depolarization fields.

Recently, $BaTiO_3/SrTiO_3$ superlattices were grown,[6,7] and their dielectric properties differed considerably from those of films of the solid solution, $Sr_{1-x}Ba_xTiO_3$. These heterostructures were characterized by a relatively large lattice mismatch of 2.2% and are, thus, either strongly strained—or they contain many misfit dislocations.

Here, we have grown an alternative system, namely superlattices of alternating paraelectric $KTaO_3$ and ferroelectric $KNbO_3$ layers, with excellent crystalline quality and having a lattice mismatch below 0.5%. By comparing the present results with those reported for $BaTiO_3/SrTiO_3$ superlattices,[6,7] a distinction may be made between true "size effects" in these structures and the influence of strains. The use of $KNbO_3$ and $KTaO_3$ is further motivated by the fact that ferroelectric $KNbO_3$ is an excellent electro-optic material.[8] This and the high price of $KNbO_3$ single crystals has recently led to the production of $KNbO_3$ thin films by various methods[8–12] including pulsed laser deposition.[13,14] While the cubic perovskite $KTaO_3$ has been thoroughly investigated, renewed interest has arisen due to the use of this material as a bulk substrate for high-T_c films,[15] and $KTaO_3$ thin films can also be grown by pulsed laser deposition.[16]

In the present study, (001)-oriented $KTaO_3$ substrate wafers ~1mm thick were cut from crystals grown by spontaneous nucleation and polished with a KOH-buffered solution of colloidal silica (pH=11). For comparison purposes, $LaAlO_3$ and $SrTiO_3$ substrates were also used.

$KNbO_3$ and $KTaO_3$ films were grown using a KrF excimer laser (248 nm, 38 nm FWHM pulse duration) with a focused energy density of 1.5–3 J/cm^2. The pulse repetition rate was 3.3 Hz, and the growth was carried out in 100 mTorr of oxygen. The substrate-target distance was 6 cm. $KTaO_3$ and $KNbO_3$ targets were prepared from mixtures of K_2CO_3, Ta_2O_5, and Nb_2O_5 powders calcined and sintered in air. Because of the high volatility of potassium, a segmented rotating disk target was used, one-half of which consisted of the perovskite and one-half of cold-pressed KNO_3 as an extra potassium source.[17] Approximately two pulses were fired per one-half rotation of the target. Therefore, the growth rate as determined below (~1 Å per pulse) indicates that about one-half of a unit cell of the perovskite is grown between two exposures to the KNO_3 source. While all of the samples were grown at 750 °C, the correct stoichiometry could, in fact, be obtained in the wide temperature range of 650–800 °C.

The stoichiometry of single $KTaO_3$ and $KNbO_3$ films was determined by Rutherford backscattering (RBS) for the case of polycrystalline films deposited on sapphire, thereby establishing the correct stoichiometry. Epitaxial $KTaO_3$ and $KNbO_3$ films were also analyzed using RBS/ion channeling. Figure 1(a) shows the results for $KNbO_3$ grown on $KTaO_3$. the observed channeling yield of <4% shows excellent crystallinity.

The film shown in Fig. 1(a) was further analyzed by x-ray diffraction using a rotating-anode Cu $K\alpha$ x-ray source, a vertically focusing LiF monochromator, a Huber four-circle

[a]Electronic mail: qha@ornl.gov
[b]Also at Departmento de Física, Universidad de Puerto Rico, Mayagüez, Puerto Rico 00681

 0003-6951/96/68(11)/1488/3/$10.00

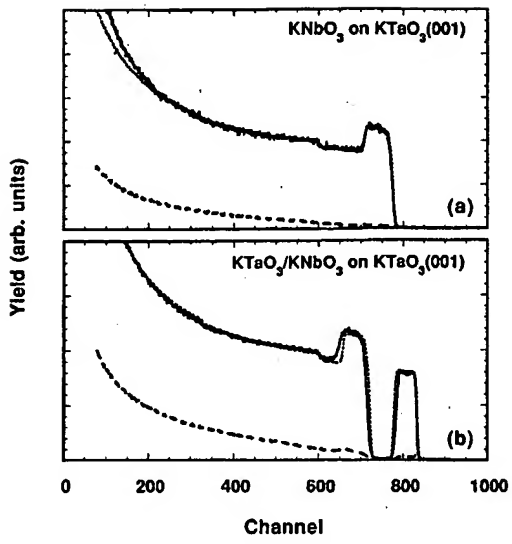

FIG. 1. RBS spectra (continuous lines) and simulated spectra (dotted lines) compared with the data obtained in the ion-channeling mode (broken lines) for: (a) $KNbO_3$ (166 nm) on $KTaO_3$, and (b) a $KTaO_3$ (144 nm)/$KNbO_3$ (146 nm) double layer on $KTaO_3$.

diffractometer, and a flat Ge analyzer crystal. The sample was mounted with the (00ℓ) axis of the substrate parallel to the Φ axis of the diffractometer. θ–2θ scans along the substrate ℓ axis are presented in Fig. 2 and show $KNbO_3$ (00ℓ) peaks associated with the $c_\perp$ orientation of the film; no additional peaks (other than the substrate reflections) are observed. The inset of Fig. 2 shows an expanded view of the (002) reflection where the interference pattern demonstrates the flatness of the film. A rocking curve across the same reflection shows a very small mosaic spread of about 0.05°.

The combined results of off-normal θ-2θ and Φ scans are consistent with an orthorhombic structure in which a=3.975 Å, b=4.001 Å (in-plane), and c=4.055 Å (along the surface normal). Following Ref. 18, Φ scans through the film's (*hhl*) reflections make it possible to distinguish between different types of in-plane epitaxy. If the a and b axes of the film were exactly aligned with the in-plane <h00> axes of the substrate, a double peak should be observed. In the case of the present films, however, a triple peak is clearly evidenced in the (222) direction. This indicates that the film's [hh0] or [$h\bar{h}$0] directions are parallel to an in-plane sub-

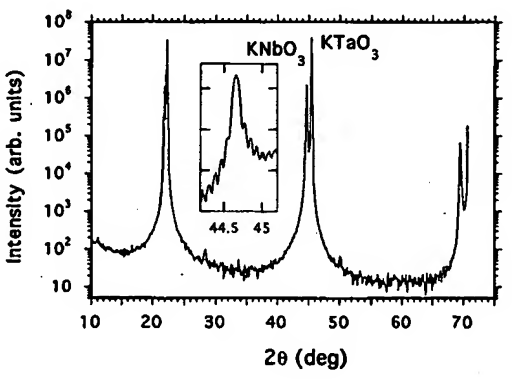

FIG. 2. X-ray θ–2θ scan along the substrate surface normal for the $KNbO_3$ film of Fig. 1(a). The inset shows an expanded view of the (002) film reflection with the interference pattern demonstrating the flatness of the film.

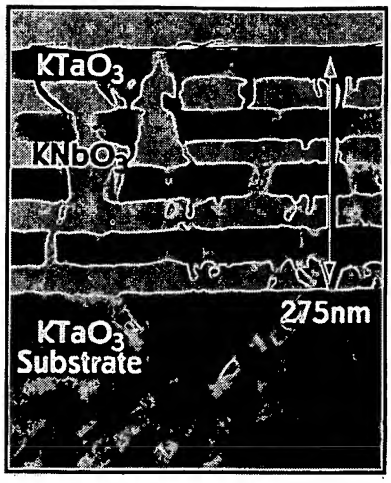

FIG. 3. Cross-sectional TEM bright field image of an 8-layer superlattice of $KTaO_3$/$KNbO_3$ on $KTaO_3$. Propagation of substrate defects through the films is clearly observed.

strate <hh0> axis. Additionally, off-normal θ-2θ scans across the film's (022) and (202) reflections reveal that the (022) peak is broader than the (202) peak. This indicates some disorder along the (022) orientation. Its origin and the consequences for the sample's physical properties remain to be investigated. It can be speculated, however, that the disorder is associated with the formation of ferroelectric domains within an orthorhombic domain.

The observed structure differs from that of bulk $KNbO_3$ ($Cm2m$ with a=5.695 Å, b=5.721 Å, and c=3.974 Å), which has been found to occur in thick films (1.5 μm). In these layers, the orthorhombic (110) orientation [i.e., the pseudocubic (001)] aligns with the substrate surface normal. Note that for the new orthorhombic structure observed for the thin films, $(a+b)/2$ equals 3.988 Å, which results in an even better lattice match (well below 0.1%) with $KTaO_3$ (a =3.989 Å) than the bulk $KNbO_3$ structure.

$KTaO_3$/$KNbO_3$ heterostructures were grown *in situ* using identical growth conditions for the two constituents. The RBS results are shown in Fig. 1(b) for a structure consisting of two layers of about 145 nm each. Reasonable agreement between the measured and simulated curves is observed, and the channeling yield shows good epitaxy for both films.

Figure 3 shows a cross-sectional transmission electron microscope (TEM) image of a structure consisting of 8 layers with thicknesses of 40 nm ($KTaO_3$) and 30 nm ($KNbO_3$). This structure was grown with 400 laser shots on the perovskite target (plus 400 shots on the $KNbO_3$ pellet) per layer, thus the growth rates are determined to be 1 and 0.75 Å per shot for $KTaO_3$ and $KNbO_3$, respectively. The micrograph shows that the dislocations, which thread through the films, originate from dislocations that were present in the substrate and are believed to arise from polishing-induced damage. These threading dislocations are responsible for the development of the surface roughness, which can be seen to increase at each succeeding film/film interface.

Z-contrast STEM[19] was used to image the $KTaO_3$/$KNbO_3$ interface with atomic resolution for a [100] zone axis oriented cross-sectioned sample. The positions of the Ta and Nb columns can be clearly distinguished and located directly

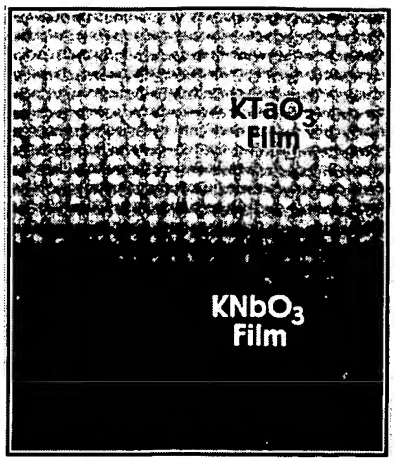

FIG. 4. Atomic-resolution cross-sectional Z-contrast scanning-TEM image of a $KTaO_3/KNbO_3$ interface in the superlattice structure of Fig. 3. Contrary to that conventional image, the brighter portion here corresponds to $KTaO_3$.

from the image (Fig. 4). The $KTaO_3/KNbO_3$ interface width, as deduced from the change in the feature intensities, is seen to be limited to one or two unit cells. This is believed to be the result of interface roughness, which exceeds a few unit cells over a length scale comparable to the thickness of the TEM specimen.

The present combined results of Z-contrast STEM, x-ray diffraction, RBS, and ion channeling demonstrate that high-quality $KTaO_3/KNbO_3$ superlattices can be grown by pulsed laser deposition. With the exception of the surface roughness (here mainly caused by substrate defects), the interfaces are extremely sharp, and the fabrication of superlattices with a much smaller periodicity is a straightforward extension of this work. The properties of the new orthorhombic structure of $KNbO_3$ when "clamped" to the $KTaO_3$ substrate template are not known at present, but their preferential structural disorder in one direction may be an indication of a polar (most likely ferroelectric) state. With the excellent lattice match between these two materials, it should be possible to study size effects on the polar behavior of this novel phase. Efforts are currently underway to study the dielectric properties of $KNbO_3/KTaO_3$ superlattice structures by growing samples on conducting substrates.

It is our pleasure to acknowledge the help of M. J. Gardner, J. A. Kolopus, J. T. Luck, and J. O. Ramey. This work was supported in part by a grant from the Swiss National Science Foundation, the Division of Materials Sciences, U.S. Department of Energy under Contract DE-AC05-84OR21400 with Lockheed Martin Energy Systems, Inc., the DOE-EPSCOR under Grant DE-FG02-94ER75764, and the NSF-EPSCOR under Grant EHR-9108775.

[1] J. G. Bednorz and K. A. Müller, Phys. Rev. Lett. **52**, 2289 (1984).
[2] H.-M. Christen, U. T. Höchli, A. Châtelain, and S. Ziolkievicz, J. Phys. Condens. Matter **3**, 8387 (1991).
[3] S. Marais, V. Heine, C. Nex, and E. Salje, Phys. Rev. Lett. **66**, 2480 (1991).
[4] P. Ayyub, V. R. Palkar, S. Chattopadhyay, and M. Multani, Phys. Rev. B **51**, 6135 (1995).
[5] W. Y. Shih, W.-H. Shih, and I. A. Aksay, Phys. Rev. B **50**, 15 575 (1994).
[6] E. Wiener-Avnear, Appl. Phys. Lett. **65**, 1784 (1994).
[7] H. Tabata, H. Tanaka, and T. Kawai, Appl. Phys. Lett. **65**, 1970 (1994).
[8] T. M. Graettinger, S. H. Rou, M. S. Ameen, O. Auciello, and A. I. Kingon, Appl. Phys. Lett. **58**, 1964 (1991).
[9] G. J. Derderian, J. D. Barrie, K. A. Aitchison, P. M. Adams, and M. L. Mecartney, Mater. Res. Soc. Symp. Proc. **310**, 339 (1993).
[10] H. Endo and M. J. Cima, Mater. Res. Soc. Symp. Proc. **310**, 325 (1993).
[11] S. Schwyn Thöni, H. W. Lehmann, and P. Günter, Appl. Phys. Lett. **61**, 373 (1992).
[12] M. J. Nystrom, B. W. Wessels, D. B. Studebaker, T. J. Marks, W. P. Lin, and G. K. Wong, Appl. Phys. Lett. **67**, 365 (1995).
[13] C. Zaldo, D. S. Gill, R. W. Eason, J. Mendiola, and P. J. Chandler, Appl. Phys. Lett. **65**, 502 (1994).
[14] V. Gopalan and R. Raj, J. Am. Ceram. Soc. **78**, 1825 (1995).
[15] R. Feenstra, L. A. Boatner, J. D. Budai, D. K. Christen, M. D. Galloway, and D. B. Poker, Appl. Phys. Lett. **54**, 1063 (1989).
[16] Yu. A. Boikov, Z. G. Ivanov, A. L. Vasiliev, I. Pronin, E. Olsson, and T. Claeson (unpublished).
[17] S. Yilmaz, T. Venkatesan, and R. Gerhard-Mulhaupt, Appl. Phys. Lett. **58**, 2479 (1991).
[18] J. D. Budai, R. Feenstra, and L. A. Boatner, Phys. Rev. B **39**, 12 355 (1989).
[19] S. J. Pennycook and D. E. Jesson, Phys. Rev. Lett. **64**, 938 (1990).